

Design Consideration of Bi-Directional CLLLC Resonant Converter in Energy Storage Systems

Guangzhi Cui¹, Sheng-Yang Yu²

¹Texas Instruments, China,

²Texas Instruments, USA

Corresponding author: Guangzhi Cui, guangzhi-cui@ti.com

Speaker: Sheng-Yang Yu, seanyu@ti.com

Abstract

The bidirectional DC-DC converter plays a key role in order to realize power distribution in systems including batteries such as energy storage systems (ESS) and automotive on-board chargers. The capacitor-inductor-inductor-inductor-capacitor (CLLLC) resonant converter topology with its symmetric resonant tank, soft switching characteristics, which helps the system achieve higher efficiency and works convenient in bidirectional power flow. In this abstract, key CLLLC resonant converter design considerations in ESS are introduced. A CLLLC resonant converter prototype with rated power 3.6kW, and battery voltage 40~60 V is built to evaluate the performance which achieves 97.4% peak efficiency.

1 Introduction

A commonly used residential ESS system is illustrated in Fig.1, a high voltage DC bus is interfacing electric grid and the battery system. It is notable that 48V battery system is widely applied in residential ESS applications because of safety considerations. Therefore, isolated bidirectional topologies should be used here to realize voltage conversion from high voltage DC bus to low voltage battery system. Instead of using two stage isolated structure, such as buck/boost converter + LLC resonant converter, a single stage isolated converter can save system cost and improve power density. Among these single stage topologies, converters with soft-switching capabilities like CLLLC resonant and Dual Active Bridge (DAB) converters would be a better choice to improve the efficiency. The performance and key features have been compared in [1], and it is found that the efficiency of a DAB converter is generally lower than a CLLLC resonant converter under the same specification. Moreover, DAB converter may lose zero voltage switching (ZVS) on the active switches at light load. For CLLLC resonant converter, it could achieve soft-switching over full load range without an additional circuit and the symmetric resonant tank ensure the similar gain and resonance characteristics in both forward and reverse operation, which helps improve the efficiency and reduce the complexity of converter design. However, the gain curve of CLLLC resonant converter is flatter when

the switching frequency is higher than series resonant frequency, especially at light load condition. Therefore, design the CLLLC resonant converter to cover a wide battery voltage range while maintain high efficiency is the key challenge for CLLLC resonant converter in ESS applications. Based on its high efficiency and ZVS features, CLLLC resonant converter is a popular study topic in recent years, [2] introduce the design method of CLLLC resonant converter parameters, but it does not introduce the control scheme and experiment is verified in high battery voltage system, [3] introduces the design and control method, but it also verifies in high voltage system and do not consider the light load condition method. In this paper, the parameters design method, control algorithm of the CLLLC resonant converter and key design considerations in ESS will be discussed and analyzed. The proposed design methodology and digital control algorithms are verified using a 3.6kW prototype converter.

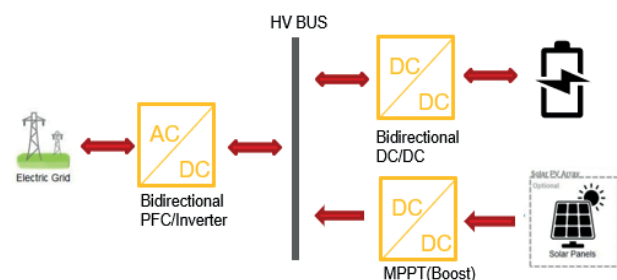


Fig. 1 Block diagram of residential ESS

2 Design methodology of bidirectional CLLC resonant converter

2.1 Design considerations of power stage

Fig. 2 shows the circuit topology of the full-bridge CLLC resonant converter. This topology consists of a symmetric resonant tank and full-bridge structure. Among the resonant tanks, the resonant inductor L_{r1} and L_{r2} could be merged with the transformer T_1 to improve the power density.

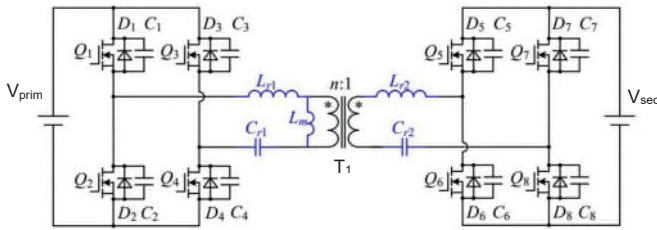


Fig.2 Schematic of CLLC resonant converter

Similar to the LLC resonant converter, FHA (First Harmonic Analysis) model could be used to analyze the CLLC resonant converter gain characteristic. The detailed operating principles and gain analysis using FHA model has been extensively researched in [2]. Based on the FHA approach, the steady-state models are obtained as shown in Fig. 3, which refer to all the resonant components from the load side to the source side. And the charging mode and discharging mode gain equation can be written as (1) and (2) using KCL and KVL.

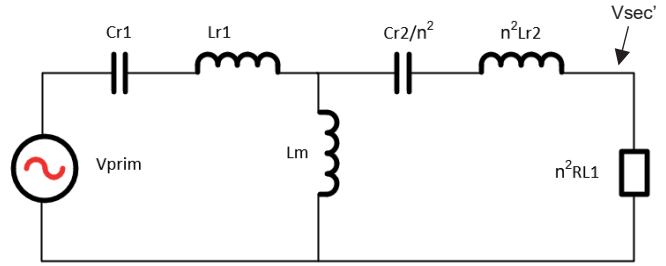
$$\frac{V_{prim}}{V_{sec}} = \frac{n * [Z_m || (Z_{r1} + R_{L1})] * R_{L1}}{(Z_{r2} + [Z_m || (Z_{r1} + R_{L1})]) * (R_{L1} + Z_{r1})} \quad (1)$$

$$\frac{V_{sec}}{V_{prim}} = \frac{R'_L * [Z_m || (Z_{r2} + R'_L)]}{n * (Z_{r1} + [Z_m || (Z_{r2} + R'_L)]) * (R'_L + Z_{r2})} \quad (2)$$

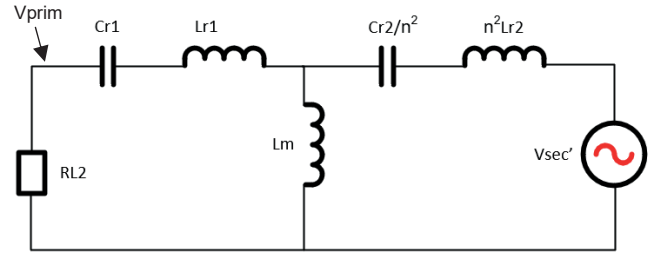
Note here the effective R_{Li} is account as

$$R_{Li} = 8 * R_{dc} / \pi^2 \quad (3)$$

Where R_{dc} is the DC resistive load at the output. V_{prim} is the voltage at primary side and V_{sec} is the voltage at secondary side as shown in Fig.3. $V_{sec'}$ is equal to $n * V_{sec}$, Z_m is equal to $s * L_m$, Z_{r1} is equal to $s * L_{r1} + 1/s * C_{r1}$, Z_{r2} is equal to $s * L_{r2} + 1/s * C_{r2}$.



(a) Battery charging mode



(b) Battery discharging mode

Fig. 3 FHA models of CLLC resonant converter

2.1.1 Design considerations of Resonant Network

Due to a wide range of battery voltage, normally ranging from 40V to 60V, the CLLC converter should work in a wide gain range. As the CLLC converter has its efficiency optimized when the switching frequency (f_{sw}) is close to the series resonant frequency (f_r), when C_{r1} & L_{r1} or C_{r2} & L_{r2} are resonant, we will have to set $f_{sw} \sim f_r$ at the operating point where maximum power is delivered. And the turn ratio of the transformer is also calculated using the same maximum power delivery point. Design of magnetizing inductor (L_m), resonant inductor (L_r), and resonant capacitor (C_r) should consider the gain range, acceptable maximum f_{sw} , soft switching conditions, and efficiency optimization. Some definitions and assumptions of the resonant tank are given by

$$k = L_m / L_{r1} \quad (4)$$

$$a = n^2 * L_{r2} / L_{r1}, \quad b = C_{r2} / (n^2 * C_{r1}) \quad (5)$$

k is the inductance ratio, a is the inductance ratio and b is the capacitance ratio. Based on the definitions, assuming a and b is equal to 1, which means the resonant tank is totally symmetrical. The gain curve with k varying is shown in Fig.4, where y-axis is the voltage gain and x-axis is the frequency.

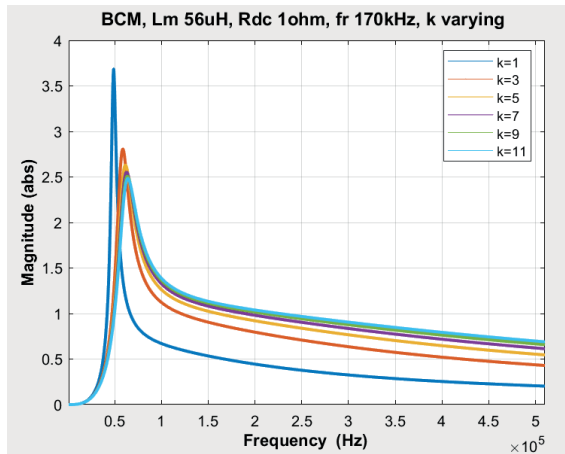


Fig. 4 Gain curve with different k value (1ohm R_{dc})

In order to cover a wide gain range, the inductance ratio k has to be low, because the peak gain is reduced with high k ratio and the gain curve will be flatter at high frequency. That is, the converter needs to operate in a wide frequency range to meet required gain. In addition, as shown in Fig.5, there will be part of non-monotonic range when frequency is lower than series resonant frequency with load current increase, which will also limit the peak gain in this situation.

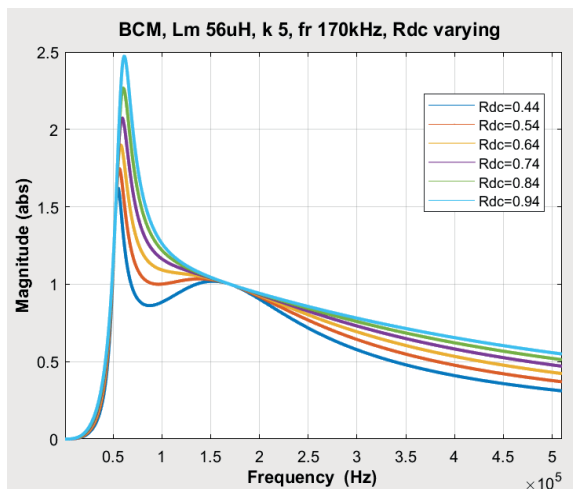


Fig.5 Gain curve with different R_{dc} value

Basically, high k means a larger L_m helps reduce circulating current to improve the efficiency, but it needs to consider if such a larger L_m could help achieve ZVS over full load range. In a resonant converter, the energy stored in magnetizing inductor L_m during the dead time is used to charge and discharge the MOSFETs output capacitance (C_{oss}) to achieve ZVS. Assuming an ideal transformer and ideal switches on the output full bridge switches (no parasitic capacitance). In order to

achieve ZVS on the input full bridge, the energy stored in L_m needs to be larger than the energy stored in all C_{oss} . Hence, the following equation must be met:

$$0.5 * L_m * I_{Lm}^2 \geq 0.5 * (4 * C_{oss}) * V_{in}^2 \quad (6)$$

$$I_{Lm} = n * V_{out} / (4 * L_m * f_{swmax}) \quad (7)$$

Actually, the transformer winding capacitance and C_{oss} capacitors of output full bridge side are non-negligible. To achieve ZVS, these parasitic capacitances should be minimized and a smaller L_m is chosen in real cases. It is recommended to verify if ZVS is achievable in the simulation model with these parasitic parameters. Besides, these parasitic capacitors will also cause non-linear gain at high frequency at light load conditions, which will be discussed in the next section.

2.1.1 Effect of resonant network's tolerance

The gain characteristic is analyzed above based on the condition $a=b=1$, the effect will be analyzed assuming $a \neq b \neq 1$ but $a*b=1$ with a certain k and R_{dc} . It means the series resonant frequency is the same in both sides but the resonant inductor and capacitor has the tolerance. Taking the different values of a and b that are listed in below table 1, the waveform in charging and discharging mode is shown in Fig.6 and Fig.7.

a	0.4	0.7	1	1.3	1.6
b	2.5	1.42	1	0.77	0.625

Table 1 value of a and b

In charging mode, if $a>1$, the gain curve is non-monotonic when frequency is lower than series resonant frequency, it is hard to regulate the output voltage by adjusting the frequency. There is no problem when $a<1$ in charging mode, but it will cause the obvious gain difference when it operates in discharging mode, the gain is flat around the series resonant frequency, which will lead to the converter operating in a wide frequency range to get high gain.

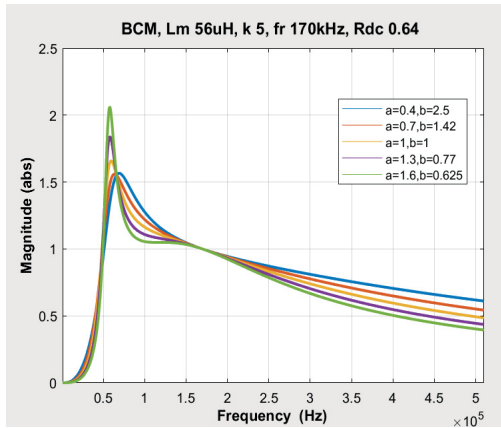


Fig. 6 Charging mode gain curve when $a*b=1$

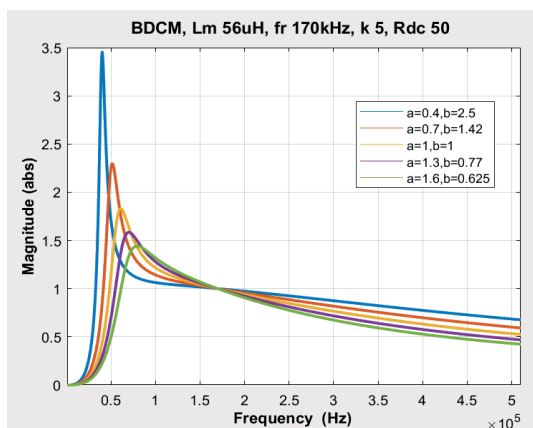


Fig. 7 Discharging mode gain curve when $a*b=1$

It is noticeable that the effect of resonant capacitor and inductor on the gain curve is different. The gain curve with constant $b=1$ and variable a is shown in Fig.8. For charging mode, when $a<1$, the tendency of the curve is similar as the one when $a=1$, but the slope increases sharply when $a>1$ at the left part of series resonant frequency.

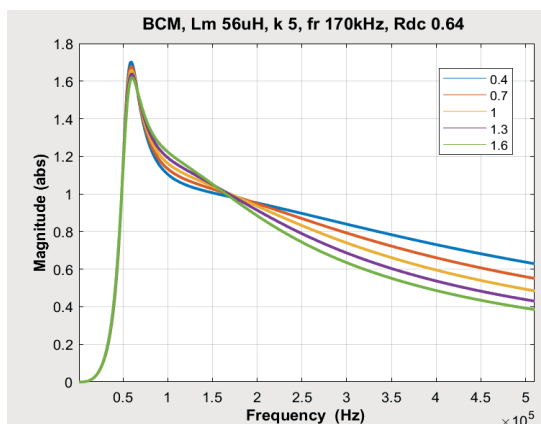


Fig. 8 Charging mode gain curve with different a

Similarly, the gain curve with constant $a=1$ and variable b could be drawn in Fig.9. According to the waveform, the tendency is similar to the one when $b=1$, but when the $b<1$, the gain curve is non-linear with the frequency decrease.

Compare Fig.8 with Fig.9, it should point out that the resonant capacitor mainly influences the part which is lower than series resonant frequency, resonant inductor mainly influences the part which is higher than series resonant frequency. Besides, the resonant capacitor has a worse effect on the gain curve, which will make the gain regulation difficult with frequency modulation below the series resonant frequency.

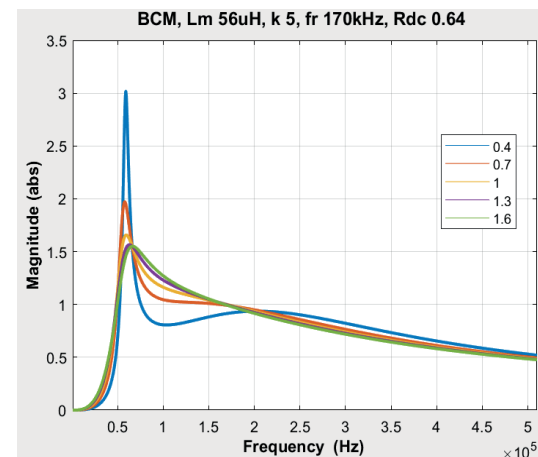


Fig. 9 Charging mode gain curve with different b

For different values of a and b , when both of them are close to 1, the gain curve in charging mode and discharging mode will be closer, the symmetry and uniformity of the converter will be better. However, it is hard to make the resonant parameters totally symmetrical in real design. Considering 20% margin of components tolerance and design error, the gain curve in different situation could be drawn in Fig.10 to Fig.13. It is found that when the tolerance of resonant parameters is within 20%, the gain curve could maintain the monotonicity in the whole frequency range. From Fig.10, the resonant inductor has a weaker effect on the gain curve, especially when the frequency is lower than series resonant frequency. From Fig.11, three gain curves coincide when the converter operates above series resonant frequency, however, it is noticeable that when the converter operates under series resonant frequency, a non-monotonic point may occur if the load continually increases. From Fig.12, when $b=0.8$ in charging mode, there will be inflection point when frequency is under resonant point, and this non-monotonic will be serious with b value decrease. In Fig.13, the gain curve seems no non-linear part but the gain curve will have ob-

vious drifting when both a and b has 20% tolerance, which will lead to gain character difference, especially at series resonant frequency. Therefore, when design the resonant parameter with $a \cdot b = 1$, which means the series resonant frequency in both sides is same, if the tolerance is within 20%, the difference is acceptable and it will not have serious effect on gain curve. Besides, it is better to control the lower end value of b within 20% to avoid the gain curve non-monotonic.

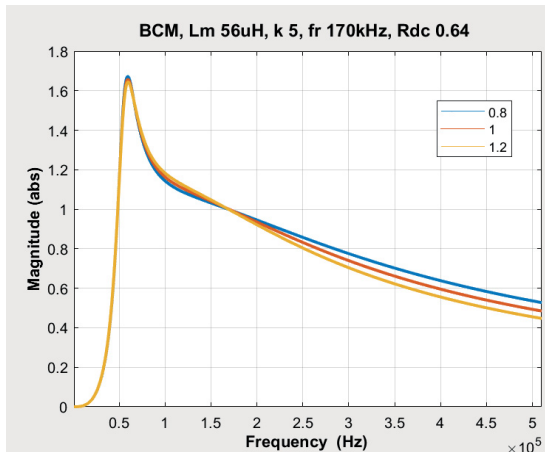


Fig. 10 Charging mode gain curve with 20% tolerance of a

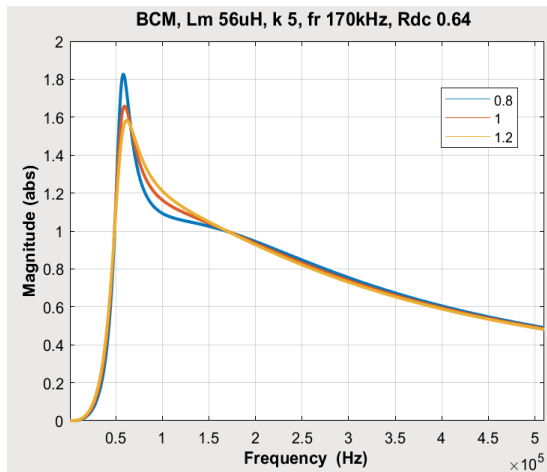


Fig. 11 Charging mode gain curve with 20% tolerance of b

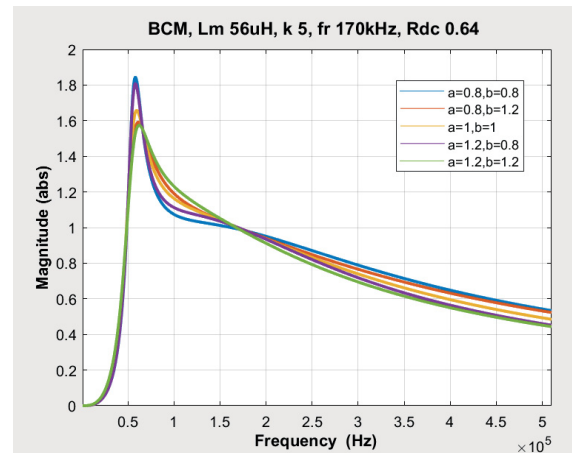


Fig. 12 Charging mode gain curve when both a and b have 20% tolerance

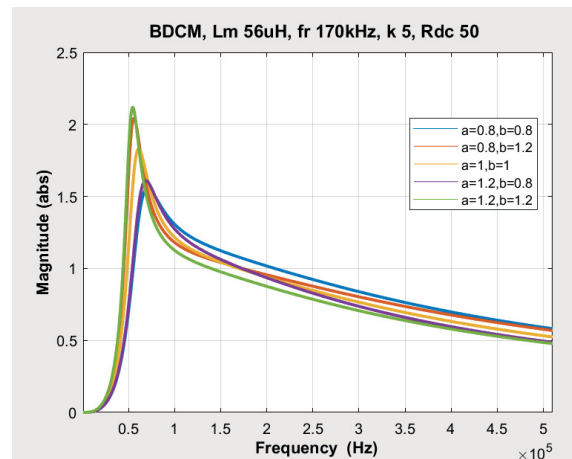


Fig. 13 Discharging mode gain curve when both a and b have 20% tolerance

2.1.2 Design methodology of resonant network

During the design procedure, the voltage gain curves should keep monotonic within the acceptable range of operating frequency and meet the voltage gain requirements at full load range in both stages. Besides, the ZVS conditions should be achieved.

1) Design of the turns ratio of transformer (n)

Because the converter operates in a wide voltage range, it is better to design the turn ratio at its typical output to achieve the maximum efficiency.

$$n = V_{bus}/V_{out_typ} \quad (8)$$

2) Calculating the maximum and minimum gain

It should calculate the maximum and minimum required gain on both sides and make sure the gain curve could cover this range. Gain equation in charging mode is shown below:

$$G_{max} = n * V_{out_max}/V_{in_min} \quad (9)$$

$$G_{min} = n * V_{out_min}/V_{in_max} \quad (10)$$

3) Design of the magnetizing inductor (L_m)

To ensure the output capacitor could be fully charged or discharged for ZVS, maximum L_m is calculated in equation (5) and (6). Basically, half of the calculated value is used because of FETs and transformer parasitic parameter effect.

4) Design of the inductor ratio (L_m/L_{r1})

Normally, a high k value helps reduce the RMS current, but the gain will decrease with k increase as shown in Fig.4, which will require wider operation frequency and be difficult to compact magnetic components design. So, select a higher k value to optimize the efficiency and make sure the gain curve could cover the calculated gain range in the specified frequency range.

5) Calculation of the resonant components

When k is defined, L_{r1} is known and C_{r1} could be calculated based on series resonant frequency. According to the analysis above, 20% tolerance of resonance is acceptable in the design but it is necessary to make sure the resonance on both sides are same ($a*b=1$). Besides, the resonant capacitor cannot be too large, as it will decrease the impedance of the resonant tank which will weaken the effect of startup current limitation at high frequency. Once the parameters are confirmed, it is recommended to do the simulation to verify the gain curve in different working conditions. Repeating the last 3 steps to find the available result if the simulation result cannot meet the specification.

2.2 Design considerations of control stage

Variable frequency control (VFC) is generally used as the CLLLC resonant converter control method. However, the gain curve is flat when $f_{sw} > f_r$, and considering the parasitic parameters of transformer intra-winding capacitance and C_{OSS} , the non-monotonic gain curve at high frequency is happening at light load. For the low voltage side, it is necessary to parallel more FETs to reduce the FET's on resistance in high power applications. In this case, the effect of C_{OSS} is serious, we can't rely just on VFC for output voltage regulation. Hiccup mode is a popular method to deal with CLLLC resonant converter non-monotonic features, but this method is not suitable in battery applications because the converter needs to deliver high current when battery voltage is low. PWM control and phase-shift control could solve this problem, but PWM control will make FETs work at hard switching state, which decreases the efficiency and limits the operation frequency. Therefore, the phase shift control is a better choice to cover this situation. The area of operations of a battery charger with variable frequency and phase-shift mixed control is proposed in Fig.14.

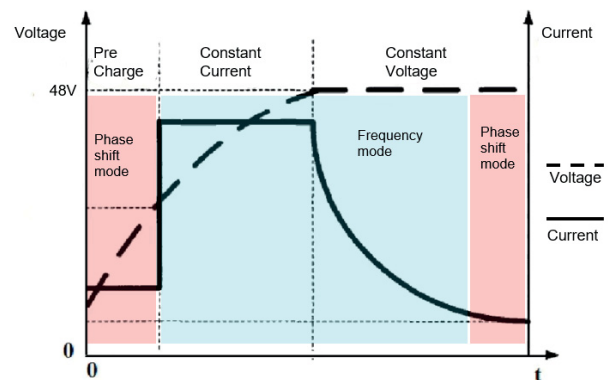


Fig. 14 Control scheme in different charge stage

During the startup stage, the output voltage is low, soft-start function is necessary to limit the high current spike if the pre-charge circuit is not used in the system. It is a limited effect to soft start from high frequency if the resonant inductor value or frequency is not high enough, so in this design the phase shift control is used as the soft start strategy. The converter will enter into frequency modulation when soft start is over. When the battery is almost fully charged, it will trickle charge with a small current and maintain a constant voltage. At this light load, output voltage tends to rise due to parasitic capacitance and could eventually go out of regulation, so the phase shift control is also needed to regulate the output voltage in this region. Whether the converter enters phase shift mode or not is decided by the controller's calculation.

tion result, Fig. 15 shows the modulation switch between frequency and phase shift. When the load decrease, the frequency will increase to regulate the output voltage, if the calculated maximum frequency is higher than the setting value, the converter will enter into phase shift modulation; then when the load increase, the phase shift angle will decrease to regulate the output voltage, the converter will enter frequency mode again when phase shift angles decreases to zero.

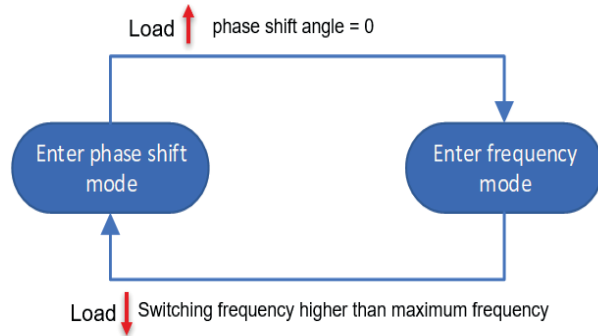


Fig. 15 Modulation switch between frequency and phase shift modes

3 Experimental results

A prototype [5] is built to verify the circuit design and performance. The transformer turns ratio $N=9$, with $L_m=56\mu\text{H}$, $L_{r1}=10\mu\text{H}$, $C_{r1}=88\text{nF}$, $L_{r2}=200\text{nH}$, $C_{r2}=4.4\mu\text{F}$. The typical input voltage and output voltage is 400V and 48V, output power is 3.6kW, series resonant frequency in 170kHz, peak efficiency in charging mode is 97.4%, in discharging mode is 95.1%. The efficiency in discharging mode is lower than charging mode, because the tank current is much higher in discharging mode when converting the primary tank current to secondary side with transformer turns ratio, which means higher condition loss in transistors and wire loss in transformer. In addition, Si FETs were used in the secondary side, compared with the GaNFETs used in the primary side, it has higher turn off loss and the increment of conduction resistance is larger with the junction temperature increasing. The efficiency test result is shown in Fig. 16, soft start waveform is shown in Fig. 17 and frequency/phase shift modulation switch test is shown in Fig. 18. From the test waveforms, the startup current is limited within 28A with 750W output power. The converter could change the modulation smoothly in different working conditions.

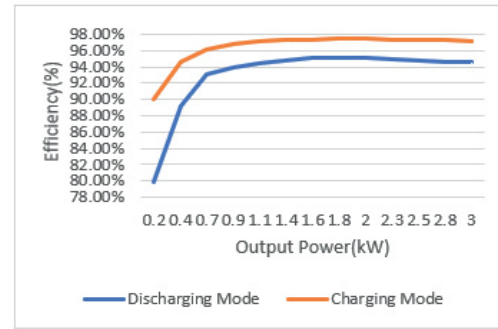


Fig. 16 Efficiency test result

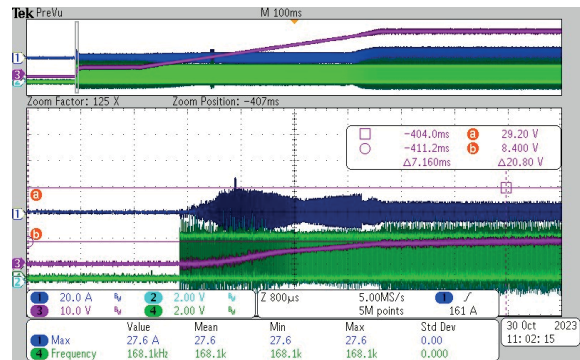
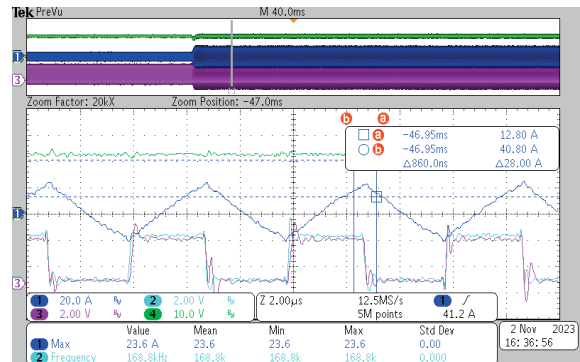
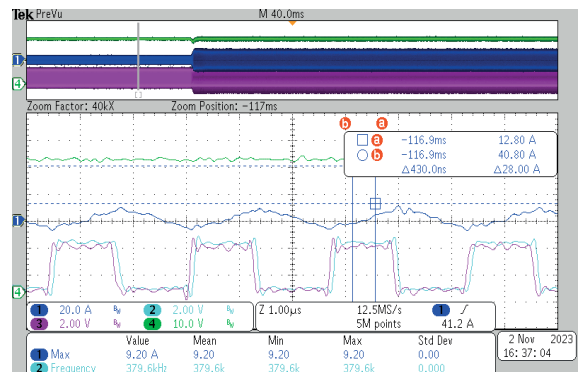


Fig. 17 Phase shift soft start with 750W output power



(a) Working at frequency mode with 5A load



(b) Working at phase shift mode with 1A load

Fig. 18 Phase shift and frequency modulation switch

4 Summary

The bidirectional CLLLC resonant converter can achieve ZVS under full load range, which reduces the switching loss and improves the system efficiency. Also, the operation principle is similar in both directions and the parameters are easy to design because of its symmetrical structure. In this paper, the design considerations of the power stage and control stage are analyzed and the design steps are also discussed. Experimental data using 3.6kW prototype verify the validity of proposed methodology and control algorithm. The maximum efficiency is 97.4% in charging mode and 95.1% in discharging mode.

References

- [1] S. -Y. Yu, C. Hsiao and J. Weng, "A High Frequency CLLLC Bi-directional Series Resonant Converter DAB Using an Integrated PCB Winding Transformer," *2020 IEEE Applied Power Electronics Conference and Exposition (APEC)*, New Orleans, LA, USA, 2020, pp.1074-1080.
- [2] H. -T. Chang, T. -J. Liang and W. -C. Yang, "Design and Implementation of Bidirectional DC-DC CLLLC Resonant Converter," *2018 IEEE Energy Conversion Congress and Exposition (ECCE)*, Portland, OR, USA, 2018, pp. 2712-2719.
- [3] J. -H. Jung, H. -S. Kim, M. -H. Ryu and J. -W. Baek, "Design Methodology of Bidirectional CLLC Resonant Converter for High-Frequency Isolation of DC Distribution Systems," in *IEEE Transactions on Power Electronics*, vol. 28, no. 4, pp. 1741- 1755, 2013.
- [4] L. Qu, X. Wang, D. Zhang, Z. Bai and Y. Liu, "A High Efficiency and Low Shutdown Current Bidirectional DC-DC CLLLC Resonant Converter," *2019 22nd International Conference on Electrical Machines and Systems (ICEMS)*, Harbin, China, 2019, pp. 1-6.
- [5] Guangzhi Cui, "Bidirectional CLLLC Resonant Converter Reference Design for Energy Storage System," *Texas Instruments Reference Design PMP41042*, 2024